IEEE Access
Multidisciplinary | Rapid Review | Open Access Journal

Received March 10, 2020, accepted April 10, 2020, date of publication April 16, 2020, date of current version May 1, 2020.

Digital Object Identifier 10.1109/ACCESS.2020.2988299

Design and Evaluation of a T-Shaped Adaptive Impedance Matching System for Vehicular Power Line Communication

BINGTING WANG[1,2], (Graduate Student Member, IEEE), ZIPING CAO[1], AND FEI SONG[1]
[1]College of Telecommunications and Information Engineering, Nanjing University of Posts and Telecommunications, Nanjing 210003, China
[2]College of Mechanical and Electrical Engineering, Chuzhou University, Chuzhou 239000, China

Corresponding author: Ziping Cao (caozp@njupt.edu.cn)

This work was supported in part by the Postgraduate Research and Practice Innovation Program of Jiangsu Province under Grant KYCX18_0888, in part by the National Natural Science Foundation of China under Grant 61372044, and in part by the Natural Science Foundation of the Jiangsu Higher Education Institutions of China under Grant 14KJA510002.

ABSTRACT The quality of the communication links in VPLC (vehicular power line communication) suffer from an impedance mismatch resulting from fluctuating VPLN (Vehicular Power Line Network) access impedance, which renders the fixed impedance matching circuit inefficient. In this paper, we designed a T-shaped adaptive impedance matching system on the basis of the resonance- and absorption-based T-shaped network complex impedance matching approach. We identified the load-Q (quality factor) for different matching situations to facilitate designing T-shaped networks with broad bandwidths. The designed T-shaped adaptive impedance matching system adjusts the component values of the T-shaped network to implement adaptive impedance matching between the VPLC modem and VPLN. A set of simulations are conducted for 1 MHz-100 MHz, which demonstrates that the designed adaptive matching system with a simple circuit structure and control logic is capable of significantly improving signal power transfer.

INDEX TERMS Impedance matching, maximum power transfer, T-shaped network, resonance and absorption.

I. INTRODUCTION

Power line communication (PLC [1]) technology is one of the most economical forms of data transmission because it uses existing power lines as the communication medium. PLC technology has been widely applied in electricity distribution grid applications. Recently, an influx of electronic devices and sensors connected to the direct current (DC) power supply of vehicles has significantly increased the weight and complexity of the wiring harness [2]. Vehicular power line communication (VPLC) can reduce the cost and installation complexity of the wiring harnesses by using existing harnesses as the transmission medium [2], [3].

However, there are many challenges that prevent the reliable and efficient communication over vehicular power lines [4]–[8]. Some of the challenges include the impulsive noise of the connected electrical components. Additionally, the location- and time-variant nature of VPLN (Vehicular Power Line Network) access impedance is caused by unpredictable load conditions. However, the fluctuating VPLN access impedance causes the impedance mismatch between the VPLC modem and the VPLN, which degrades signal power transfer and affects communication reliability. To address these problems, a new impedance matching circuit is needed.

In [9], impedance matching approaches like the optimal winding ratio selection method were explored. In this example, a coupling transformer achieved impedance matching by varying winding ratios. The practical implementation of a low-cost impedance matching circuit is presented in [10]. To address the cost issue, L-C band-pass matching couplers [11]–[13] were used as alternatives to coupling transformers, which include a BPF (Band Pass Filter) circuit and an impedance matching circuit. In cases where matching a resistive load to a resistive source is considered, band-pass matching circuits often have fixed structures and components. This means that the circuits cannot achieve dynamic impedance matching. In VPLN, access impedance

The associate editor coordinating the review of this manuscript and approving it for publication was Jenny Mahoney.

is a complex-valued quantity and varies with location and time [6], [14]; thus, a lack of dynamic impedance matching results in inefficient fixed matching circuits that require adaptive impedance matching.

Other studies considered finding adaptive impedance matching solutions. For example, in [15], an impedance matching circuitry based on a voltage-controllable inductance circuit, composed of resistors, capacitors and OP-Amps, was proposed to integrate circuits without using bulky passive inductors. In [16], a band-pass impedance matching circuit performed impedance matching via a microcontroller, an active inductor and a digital capacitor; this was done to adjust the resistive and reactive components, which matched the source and load impedances. However, these two adaptive matching approaches use off-chip transformers that increase the size, weight and cost of the system. To address this problem, articles [8] and [17] achieved adaptive impedance matching by adjusting circuit structure and component values of the L-shaped networks. A single L-shaped network has only two variable components, which restricts the network's impedance matching capabilities, and is able to achieve impedance matching over a limited Smith Chart region [18]–[21]. There are forbidden regions in the Smith Chart for a single L-shaped network. The Smith Chart was divided into eight regions. The access impedances located at different regions can not be matched by a single L-shaped network of fixed structure. To cover a larger area in the Smith chart, the L-shaped adaptive matching system needs to adjust the structure of L-shaped network to suit the impedance with different regions. Therefore, the L-shaped adaptive matching system increases the impedance-matching unit structure and necessitates additional control signals to adjust the matching network's structure for impedance adaptation. Furthermore, an ideal L-shaped network with tunable capacitors and tunable inductors was used to implement the impedance matching unit for the L-shaped adaptive matching system. However, there is no practical tunable inductor available [18]. Further, the available tunable capacitors with finite tuning ranges fail to satisfy the requirements of impedance adaptation.

Unlike the L-shaped network, the T-shaped network can achieve impedance matching for any given load impedance (without forbidden region). In this study, we designed a T-shaped adaptive impedance-matching system to enable impedance matching over a wide matching region without changing its circuit structures. Furthermore, we provided a solution to the implementation of the T-shaped impedance-matching unit. Capacitor arrays with a growing factor of 2^{i-1} are used to achieve the equivalent tunable capacitors. To reduce the cost and size of the T-shaped adaptive system, the active inductor, e.g., a General Impedance Converter (GIC), serves as an equivalent tunable inductor to avoid using bulky passive inductors. The designed T-shaped adaptive matching system has a simple circuit for impedance-matching unit, because it achieves impedance matching without adjusting its circuit structure (typology). Thus, it reduces the circuit complexity (control logic), system size and implementation cost.

For VPLC, the impedance of modem is a real-valued quantity while the VPLN access impedance is a complex-valued quantity. First, to achieve impedance matching between VPLC modem and VPLN, we illustrated a complex impedance matching approach for the T-shaped network based on circuit resonance and absorption characteristics. Second, we designed a T-shaped adaptive impedance matching system based on the T-shaped network complex impedance matching approach. Finally, we performed impedance matching at both the transmitter-side and receiver-side to investigate the performance (1 MHz-100 MHz) of our T-shaped impedance matching network via a series of simulations. The T-shaped impedance matching networks exhibit a similar power transfer performance as the L-shaped networks.

The remainder of this paper is organized as follows. Section II introduces four typical three-element matching networks and analyzes their applicability for VPLC. Then, a real-to-real impedance matching approach is presented. Section III details the resonance- and absorption-based T-shaped network complex impedance matching approach. Section IV illustrates the design process and the resulting adaptive impedance matching system circuits. Section V reviews and analyzes the simulation results. Section VI provides a summary of the work and suggests future research directions.

II. THREE-ELEMENT MATCHING NETWORKS AND REAL-TO-REAL IMPEDANCE MATCHING APPROACH

In [21]–[25], the authors investigated three-element Π- and T-shaped matching techniques. In [26]–[28], the authors describes a Q-based real-to-real impedance matching approach to achieve impedance matching between a resistive source and a resistive load for Π- and T-shaped networks.

However, the VPLN access impedance is a complex-valued quantity, which has real and imaginary impedance components. Unlike L-shaped networks, Π- and T-shaped networks have three variable components, but only two equations are provided to describe the complex-valued impedance (i.e., the real and imaginary impedance components). Thus, there is no unique solution to the component values of the T-shaped (or Π-shaped) network for matching the complex-valued impedance [21], [24]. To achieve impedance matching between the VPLC modem and the VPLN, a complex impedance matching approach for Π- and T-shaped networks should be proposed.

In the following sections, we first discuss why we choose the high-pass T-shaped network, and then describe the Q-based real-to-real impedance matching approaches [26]–[28]. We will illustrate the resonance- and absorption-based T-shaped network complex impedance matching approach in Section III.

A. TYPICAL THREE-ELEMENT NETWORKS AND THEIR APPLICABILITY

As shown in Fig. 1, typical three-element networks are the Π- and T-shaped networks, which are separated into low- and high-pass categories.

As in AC-PLC (Alternating Current-Power Line Communication), injecting or extracting communication signals from VPLN require VPLC couplers (interface circuits). On the one hand, VPLC couplers could possess the coupling function to filter the power waveform that could damage the

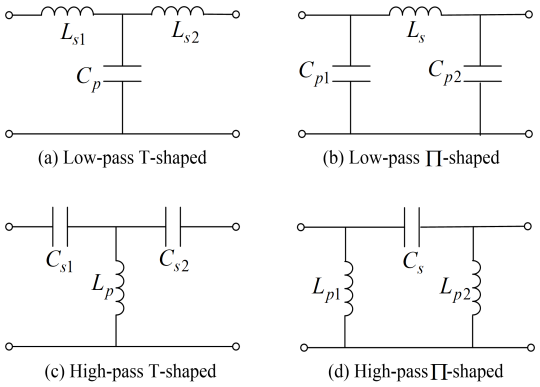

FIGURE 1. Typical three-element matching networks (a) Low-pass T-shaped; (b) Low-pass Π-shaped; (c) High-pass T-shaped; (d) High-pass Π-shaped.

communication devices or modems. On the other hand, VPLC couplers could possess impedance matching capabilities to maximize the signal power transfer. Since the supply currents and communication signals and noises exist in the same power line channel, in addition to impedance matching, the matching network (coupler) has another important task: to filter the power waveform that could damage the communication devices or modems [13].

As shown in Fig. 1(a) and (b), the DC power waveform will short-circuit the series inductors (L_{s1}, L_{s2} and L_s), which will draw large currents from the VPLN and further damage VPLC devices and modems. Therefore, the low-pass Π- and T- shaped networks should not be applied in VPLC applications. As shown in Fig. 1(d), the parallel inductor L_{p2} (or L_{p1}) will also be short-circuited by a DC power signal introduced from the VPLN (or transmitter-side), which will also draw large currents from the VPLN (or transmitter-side) and damage the inductors. Therefore, the high-pass Π-shaped network cannot be applied in the VPLC.

In this work, we investigate the high-pass T-shaped network (see Fig. 1(c)), where the series capacitor C_{s2} (or C_{s1}) is used as a coupling circuit to block the DC power waveform from damaging the communication devices or circuit components. In [29], the 12-V low-voltage VPLN is obtained by a 48-V to 12-V DC-DC converter that feeds all peripherals (other electronics devices and lights in vehicles). For a 12-V_{rms} (17-V_{peak}) VPLN, the capacitor C_{s2} (or C_{s1}), rated as a 36-V capacitor, can be used to couple and isolate the VPLN power waveform.

B. THE REAL-TO-REAL IMPEDANCE MATCHING

As shown in Fig. 2(a), V_s and R_s are the output voltage and internal resistance of the signal source, respectively. The source impedance R_s is 50 Ω, and the R_{acc} is the real-valued load impedance. The Q-based T-shaped network real-real impedance matching approach [26]–[28] can be used to achieve impedance matching between a resistive source and a resistive load. To achieve the real-to-real impedance matching, the T-shaped matching network needs to be broken into

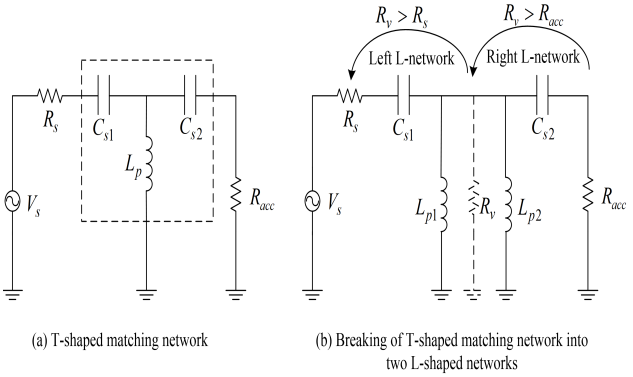

FIGURE 2. The T-shaped matching network shown as two-cascaded L-shaped networks.

two back-to-back L-shaped networks, as shown in Fig. 2(b). The impedance matching between R_s and R_{acc} is transformed to match the R_s and R_{acc} to a "virtual" resistance R_v located at the junction between the two L-shaped networks. The "virtual" resistance R_v is determined by the desired load quality (load-Q) factor and must be larger than either R_s or R_{acc} because it is parallel to the shunt leg of each L-network. The "virtual" resistance R_v [27], [28] can be calculated via the expression

$$R_v = (1 + Q^2)R_{small}, \tag{1}$$

where $Q = \frac{f_0}{BW}$ is the load-Q factor of the matching network determined by the operating frequency f_0 and bandwidth BW. R_{small} is the smallest terminating impedance of R_s and R_{acc}.

After the "virtual" resistance R_v has been obtained, the real-to-real impedance matching process is achieved via two consecutive L-shaped network-impedance matching processes.

As shown in Fig. 2(b), for the left L-shaped matching network, the Q-factor is characterized by the expression

$$Q_{left} = \sqrt{\frac{R_v}{R_s} - 1}. \tag{2}$$

The Q-factor can also be expressed as the ratio of reactance to resistance, as in

$$\begin{aligned} Q_{left} &= \frac{X_{s1}}{R_s} \\ &= \frac{R_v}{X_{p1}}, \end{aligned} \tag{3}$$

where X_{s1} and X_{p1} are the reactance of the capacitance C_{s1} and the inductance L_{p1}. Then, the values of C_{s1} and L_{p1} can be calculated via

$$\begin{cases} C_{s1} = \dfrac{1}{\omega_0 X_{s1}} = \dfrac{1}{\omega_0 R_s Q_{left}}, \\ L_{p1} = \dfrac{X_{p1}}{\omega_0} = \dfrac{R_v}{\omega_0 Q_{left}}. \end{cases} \tag{4}$$

For the right L-shaped matching network, the Q-factor is characterized by

$$\begin{aligned} Q_{right} &= \sqrt{\frac{R_v}{R_{acc}} - 1}, \\ &= \frac{X_{s2}}{R_{acc}} = \frac{R_v}{X_{p2}}, \end{aligned} \tag{5}$$

where X_{s2} and X_{p2} are the reactance of the capacitor C_{s2} and the inductor L_{p2}, respectively. Then, the values of C_{s2} and L_{p2} can be expressed as

$$\begin{cases} C_{s2} = \dfrac{1}{\omega_0 X_{s2}} = \dfrac{1}{\omega_0 R_{acc} Q_{right}}, \\ L_{p2} = \dfrac{X_{p2}}{\omega_0} = \dfrac{R_v}{\omega_0 Q_{right}}. \end{cases} \tag{6}$$

For a real-valued source impedance ($R_s = 50\,\Omega$), when a real-valued load impedance (R_{acc}) and a desired load-Q are given, a T-shaped matching network can be constructed according to Eqs. (1)-(6).

III. OUR IMPEDANCE MATCHING APPROACH FOR THE TRANSMITTER-RECEIVER CHAIN

In this section, we first introduce the VPLC model and describe our impedance matching approach and its associated system's structure.

A. VEHICULAR POWER LINE COMMUNICATION MODEL

The VPLC model is shown in Fig. 3. It includes three components: the transmitter, the in-vehicle power line network, and the receiver.

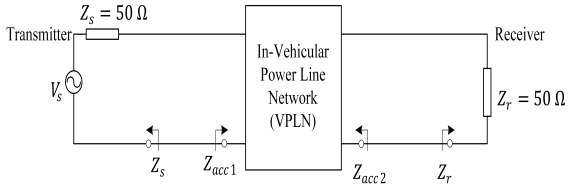

FIGURE 3. Vehicular power line communication model.

At the transmitter, V_s and Z_s are the voltage and internal impedance of the source, respectively. At the in-vehicle power line network, the VPLN is made up of wiring harnesses, electronic devices and the lights. The network can be modeled as a two-port network and the VPLN access impedance (Z_{acc}) can be characterized by the Thevenin/Norton equivalent impedance. At the receiver, Z_r represents the input impedance of the receiver.

The VPLN access impedance ($Z_{acc} = R_{acc} \pm jX_{acc}$) is a complex-valued quantity that varies with time and location. However, the impedance for transmitters or receivers, e.g., 50 Ω, can result in impedance mismatch between the VPLC modem (transmitter/receiver) and the VPLN that leads to signal reflection and degradation.

To maximize signal power transfer, the impedance matching between VPLC modem and VPLN needs to be investigated. In the following work, we illustrate the resonance- and absorption-based complex impedance matching approach for T-shaped network (see Section III–B), discuss the selection of load-Q (see Section III–C) and introduce the adaptive impedance matching system structure (see Section III–D). The design process of the T-shaped adaptive matching system is detailed in Section IV.

B. THE RESONANCE- AND ABSORPTION-BASED COMPLEX IMPEDANCE MATCHING APPROACH

The real-to-real impedance matching approach for T-shaped network is detailed in Section II-B. However, the VPLN access impedance is a complex-valued quantity (has real and imaginary impedance components). To achieve impedance matching between the VPLC modem and the VPLN, a T-shaped matching network is designed based on circuit resonance and absorption characteristics.

1) THE IMPEDANCE MATCHING FOR INDUCTIVE ACCESS IMPEDANCE

As shown in Fig. 4, V_s and R_s are the voltage and output impedance of the VPLC transmitter (modem), respectively. The output impedance of the transmitter (R_s) is 50 Ω.

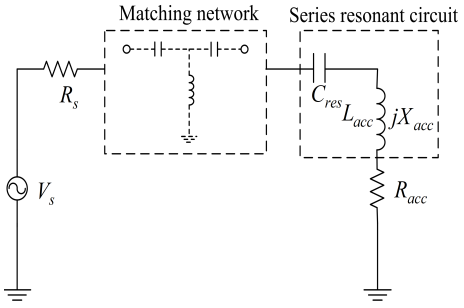

FIGURE 4. The series resonant circuit for an inductive access impedance.

To transform the complex impedance matching to a real-to-real impedance matching process, we should transform the complex-valued VPLN access impedance to a real-valued quantity. As shown in Fig. 4, when the access impedance is inductive (e.g., $Z_{acc} = R_{acc} + jX_{acc}$), the imaginary part of the VPLN access impedance can be represented by the reactance of inductance L_{acc} ($\omega_0 L_{acc} = X_{acc}$). The VPLN access impedance can also be represented by a combination of the resistance R_{acc} and inductance L_{acc}.

In a series-resonant circuit (shown in Fig. 4), when the resonance occurs ($\frac{1}{\omega_0 C_{res}} = \omega_0 L_{acc}$), the reactance of the series capacitance (C_{res}) and the inductance (L_{acc}) cancel each other out. Therefore, remaining the real part (R_{acc}) of the VPLN access impedance. The series resonant capacitance can be calculated via the expression

$$C_{res} = \frac{1}{\omega_0 X_{acc}}, \tag{7}$$

where $\omega_0 = 2\pi f_0$ is the resonant frequency, and X_{acc} is the imaginary part of the VPLN access impedance.

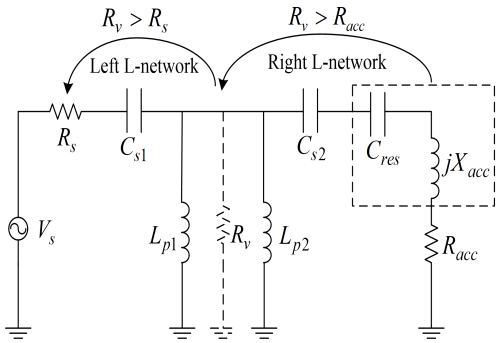

FIGURE 5. Impedance matching for inductive access impedance.

Next, as shown in Fig. 5, the complex impedance matching process is transformed to a real-to-real impedance matching (between R_{acc} and R_s) by canceling the imaginary part of the VPLN access impedance. The T-shaped matching network can then be created by the real-to-real impedance matching process shown in Section II-B.

Finally, the T-shaped matching network can be obtained by absorbing the series resonant capacitance C_{res} into the T-shaped matching network. Because the C_{res} and C_{s2} are connected in-series, the total series capacitance is $C_{eq} = \frac{C_{res} \times C_{s2}}{C_{res} + C_{s2}}$.

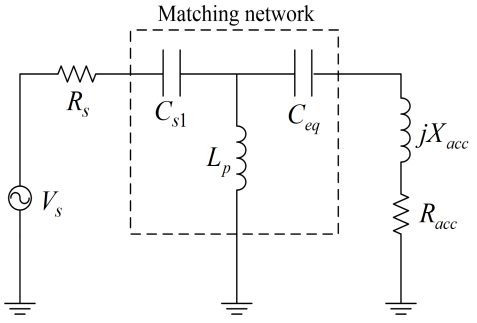

FIGURE 6. The final T-shaped matching network for inductive access impedance.

The final T-shaped matching network, for inductive access impedance, is shown in Fig. 6. The values of the T-shaped matching network components are obtained by using the following system of equations:

$$\begin{cases} C_{s1} = \dfrac{1}{\omega_0 R_s Q_{left}}, \\ L_p = \dfrac{L_{p1} \times L_{p2}}{L_{p1} + L_{p2}}, \\ C_{eq} = \dfrac{C_{s2} \times C_{res}}{C_{s2} + C_{res}}. \end{cases} \tag{8}$$

When an inductive VPLN access impedance ($Z_{acc} = R_{acc} + jX_{acc}$) and a desired load-Q are known, the T-shaped matching network can be designed via Eqs. (1)-(8). This is shown in Fig. 6.

2) THE IMPEDANCE MATCHING FOR CAPACITIVE ACCESS IMPEDANCE

When the VPLN access impedance is capacitive, e.g., $Z_{acc} = R_{acc}$-jX_{acc}, the imaginary part of the VPLN access impedance can be represented by the reactance of capacitance C_{acc}, as shown in Fig. 7. The value of the capacitance can be calculated via the expression

$$C_{acc} = \frac{1}{\omega_0 X_{acc}}. \tag{9}$$

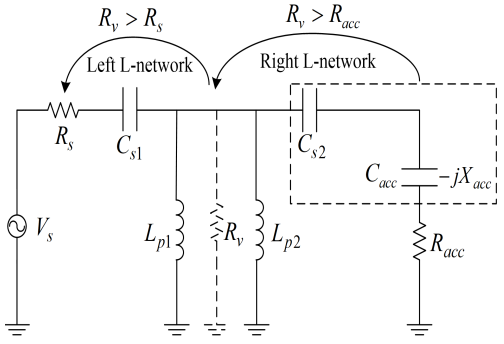

FIGURE 7. Impedance matching for capacitive access impedance.

As shown in Fig. 7, the VPLN access impedance can be represented by a combination of the resistance R_{acc} and capacitance C_{acc}. First, we should achieve the real-to-real impedance matching between R_{acc} and R_s to form a T-shaped network, which is detailed in Section II-B.

Next, the capacitance C_{acc} should be canceled, i.e., removed from the capacitance C_{s2} in the T-shaped matching network.

Finally, the T-shaped matching network for capacitive access impedance is shown in Fig. 8. The figure shows where the total series capacitance of C_{eq} and C_{acc} is equal to C_{s2} (that is $C_{s2} = \frac{C_{eq} \times C_{acc}}{C_{eq} + C_{acc}}$).

The values of the final T-shaped matching network components are calculated by using the following system of

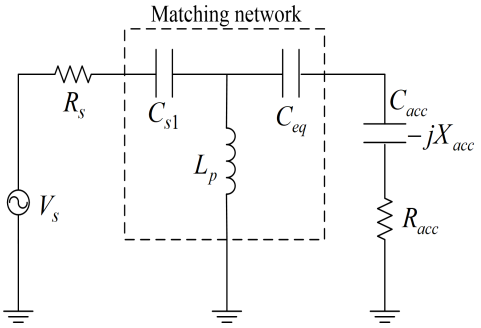

FIGURE 8. The final T-shaped matching network for capacitive access impedance.

equations:

$$\begin{cases} C_{s1} = \dfrac{1}{\omega_0 R_s Q_{left}}, \\ L_p = \dfrac{L_{p1} \times L_{p2}}{L_{p1} + L_{p2}}, \\ C_{eq} = \dfrac{C_{acc} \times C_{s2}}{C_{acc} - C_{s2}}. \end{cases} \tag{10}$$

For a given capacitive VPLN access impedance ($Z_{acc} = R_{acc}$-jX_{acc}) and a desired load-Q, the T-shaped matching network is designed by using Eqs. (1)-(6) and Eqs. (9)-(10). This is shown in Fig. 8.

C. THE SELECTION OF THE LOAD-Q

As discussed in Section II-B and Section III-B, aside from knowing the VPLN access impedance (R_{acc} and X_{acc}), the load-Q is another important parameter used to design a T-shaped impedance matching network.

1) THE LOAD-Q FOR INDUCTIVE ACCESS IMPEDANCE

In Section II-B, the calculation processes of the T-shaped matching networks are based on the condition of the "virtual" resistance R_v. This quantity must be larger than either R_s or R_{acc}. When the VPLN access impedance is inductive, for the $R_{acc} > R_s$ case, the $R_v = (1+Q^2) \times R_s$ must be larger than R_{acc}. Therefore,

$$Q > \sqrt{\frac{R_{acc}}{R_s} - 1}. \tag{11}$$

For the $R_{acc} < R_s$ case, the $R_v = (1 + Q^2) \times R_{acc}$ must be larger than R_s. Therefore,

$$Q > \sqrt{\frac{R_s}{R_{acc}} - 1}. \tag{12}$$

2) THE LOAD-Q FOR CAPACITIVE ACCESS IMPEDANCE

In addition to the condition that R_v must be larger than either R_s or R_{acc}, $C_{acc} > C_{s2}$ ($C_{eq} > 0$ in Eq. (10)) should be satisfied as well. Therefore, when the VPLN access impedance is capacitive, the load-Q for $R_{acc} > R_s$ and $R_{acc} < R_s$ cases should be limited by Eq. (13) and Eq. (14), respectively.

$$\begin{cases} Q > \sqrt{\dfrac{R_{acc}}{R_s} - 1}, \\ \qquad\qquad for\ R_{acc} > R_s \\ Q > \sqrt{\dfrac{X_{acc}^2 + R_{acc}^2}{R_s R_{acc}} - 1}, \end{cases} \tag{13}$$

$$\begin{cases} Q > \sqrt{\dfrac{R_s}{R_L} - 1}, \\ \qquad\qquad for\ R_{acc} < R_s \\ Q > \dfrac{|X_{acc}|}{R_{acc}}, \end{cases} \tag{14}$$

The conditions (Eqs. (11)-(14)) represent the minimum load-Q (Q_{min}) achievable with a T-shaped network impedance matching. The Eqs. (13)-(14) also represent the limits where the capacitor $C_{eq} = 0$ and the three-element T-shaped matching network reduces to a two-element L-shaped network. The $C_{eq} = 0$ is not allowed because the capacitor C_{eq} is used 1) as a coupling circuit to block the power waveform and 2) to prevent the parallel inductor L_p from be short-circuited by DC power waveform from VPLN. From Eqs. (11)-(14), the load-Q of a T-shaped matching network is always larger than the load-Q of an L-shaped network; according to $Q = \frac{f_0}{BW}$, for a given matching frequency f_0, the bandwidth of a T-shaped matching network is narrower than that of an L-shaped network.

Lumped-element matching is a single-frequency matching process. When the signal frequency is equal to the matching frequency of the T-shaped matching network, the impedance mismatch between VPLC modem and VPLN is compensated by the T-shaped matching network and a maximum power transfer, or ideal matching, can be achieved. The impedance of capacitance and inductance in the T-shaped matching network varies with frequency; when the signal frequency deviates from the matching frequency, the power transfer decreases. However, the broader the bandwidth of the T-shaped matching network, the less the influence that the network's impedance fluctuation has on the power transfer. According to $Q = \frac{f_0}{BW}$, for a given matching frequency f_0, to obtain a large bandwidth of a T-shaped matching network, a smaller load-Q should be selected.

D. SYSTEM STRUCTURE

In this work, we design a T-shaped adaptive impedance matching system based on the T-shaped network complex impedance matching approach (Section III-B). The block diagram of our adaptive impedance matching system is shown in Fig. 9. In the diagram, two adaptive impedance matching systems, at the transmitter-side and receiver-side, consist of three units: the measurement unit, the control unit, and the impedance matching unit, which is similar to the structure presented in [8].

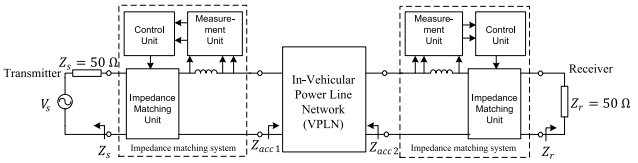

FIGURE 9. The adaptive impedance matching system for VPLC.

For our T-shaped adaptive impedance matching system, the measurement unit located between the transmitter/receiver and VPLN measures the real and imaginary parts of the VPLN access impedance. The control unit receives the outputs from the measurement unit, and calculates component values according to the resonance- and absorption-based complex impedance matching approach detailed in Section III-B. Then, it sends out the corresponding control signal to the impedance matching unit to determine the relay (or switch) status and the digital potentiometer values in the tunable capacitor and the inductor's equivalent circuit. The impedance matching unit is a T-shaped network, which adjusts the relay status and the digital potentiometer values according to the control signal provided by the control unit to achieve adaptive impedance matching.

IV. THE T-SHAPED ADAPTIVE IMPEDANCE MATCHING SYSTEM DESIGN

The T-shaped adaptive impedance-matching system includes a measurement unit, control unit, and impedance-matching unit.

The measurement unit measures the access voltage and current and provides real and imaginary parts (R_{acc} and X_{acc}) of the VPLN access impedance to the control unit for decision making. Previous scholars have presented impedance measurement circuits composed of a sensing circuit and a detector [19], [30]. A sensing circuit containing a fixed inductor and two Operational Amplifiers (Op-Amps) can be used to provide the access voltage and current of the VPLN for the detector. The detector receives the outputs from the sensing circuit, then obtains the real and imaginary parts of the VPLN access impedance.

A. IMPEDANCE MATCHING UNIT

Figure 10 shows the impedance matching unit structure (T-shaped network) that can be used for adaptive impedance matching. As illustrated in Section III–B, the actual component values of the T-shaped network can be determined via Eqs. (8) and (10) for inductive access impedance and capacitive access impedance, respectively.

An ideal T-shaped network, using tunable capacitors and tunable inductors, is shown in Fig. 10. However, there are no practical tunable inductors [18]. Furthermore, the limited tuning range of the available tunable capacitors can not satisfy the required large capacitor values in the impedance matching network. As shown in Fig. 11, capacitor arrays with growing

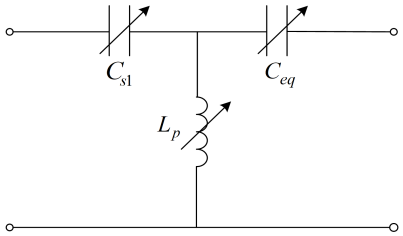

FIGURE 10. T-shaped impedance matching unit.

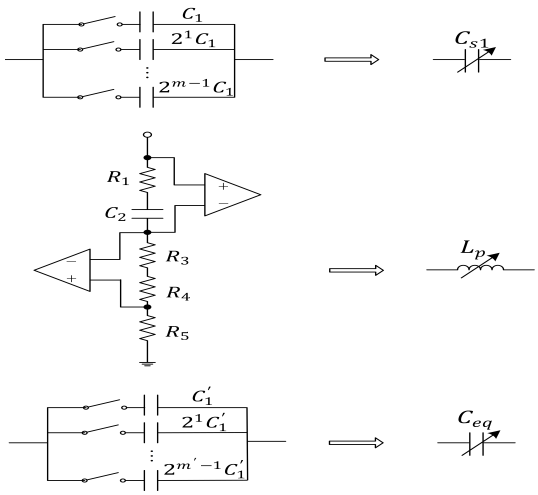

FIGURE 11. Equivalent tunable capacitor and inductor.

factor of 2^{i-1} can be used to achieve equivalent tunable capacitors. The digital relays (switches), which are controlled by the microcontroller in the control unit, determine which capacitors contribute the total values of the capacitor array. The successive approximation algorithm is applied to determine the status of the digital relays. Digital relays are used in the capacitor arrays instead of analog switches, because the latter have conduction impedance (usually several Ohms to tens of Ohms) affecting the accuracy of impedance matching in the T-type network. To avoid using bulky passive inductors, an active inductor, e.g., a General Impedance Converter (GIC [31]), is used as an equivalent tunable inductor. In addition to the two Op-Amps, the GIC consists of three resistors (R_1, R_3, and R_5), a digital potentiometer (R_4), and a capacitor (C_2) (see Fig. 11). The equivalent tunable inductor is formed by adjusting the values of the digital potentiometer (R_4) that determines the tuning range of the active inductor. The equivalent capacitance and inductance can be expressed as

$$\begin{cases} C_{s1} = \sum_{i=1}^{m} k_i C_i \qquad k_i = 0\,or\,1, \\ L_p = \dfrac{R_1 C_2 R_3 R_5}{R_4} \\ C_{eq} = \sum_{i'=1}^{m'} k_{i'} C'_{i'} \quad k_{i'} = 0\,or\,1, \end{cases} \tag{15}$$

where k_i and $k_{i'}$ represent the relay status, e.g., $k_i = k_{i'} = 0$ indicates the relays are in the open positions while $k_i = k_{i'} = 1$ indicates the relays are in the closed positions. $C_i = 2^{i-1}C_1$ and $C'_{i'} = 2^{i'-1}C'_1$ are the parallel capacitors in the equivalent tunable capacitor circuits shown in the Fig. 11. The values of C_{s1} and C_{eq} can range between $0 \sim (2^m - 1)C_1$ and $0 \sim (2^{m'} - 1)C'_1$, respectively.

B. CONTROL UNIT

The control unit includes a microcontroller, which uses the outputs from the measurement unit to calculate the components values of the T-shaped network and transmit the control signal that determines the relay status and the digital potentiometer values in the tunable capacitor and the inductor's equivalent circuit.

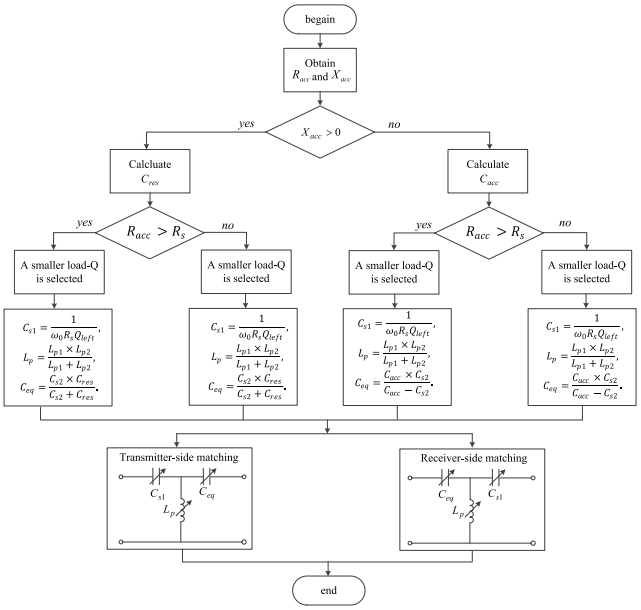

FIGURE 12. Flowchart of the proposed adaptive impedance matching solution.

The flowchart shown in Fig. 12 describes the steps used to generate the final components values of the T-shaped adaptive impedance matching system for the transmitter-side and receiver-side matching.

First, the microcontroller receives the outputs from the measurement unit to obtain the real and imaginary parts (R_{acc} and X_{acc}) of the VPLN access impedance.

Next, the microcontroller determines whether the X_{acc} is larger or smaller than zero; this is performed to determine whether the VPLN access impedance is inductive or capacitive. If $X_{acc} > 0$, the VPLN access impedance is inductive, otherwise the VPLN access impedance is capacitive.

If the VPLN access impedance is inductive ($X_{acc} > 0$), the microcontroller calculates C_{res} according to Eq. (7). It then determines whether the R_{acc} is larger than the R_s or not. If $R_{acc} > R_s$ (or $R_{acc} < R_s$), the value scope of load-Q is calculated according to Eq. 11 (or Eq. 12). A smaller load-Q was selected here to create a broadband matching network. The component values of the T-shaped network for inductive access impedance can then be calculated via Eq. (8).

Otherwise ($X_{acc} < 0$), the microcontroller calculates C_{acc} according to Eq. (9) and determines the value scope of load-Q via Eq. (13) (or Eq. (14)) for $R_{acc} > R_s$ (or $R_{acc} < R_s$) cases. A smaller load-Q can then be selected to create a broadband matching network. The component values of the T-shaped network for capacitive access impedance can be calculated by Eq. (10).

Finally, the microcontroller transmits the control signal to the impedance-matching unit to determine the relay status and digital potentiometer values in the tunable capacitor and the inductor's equivalent circuit; this determines the component values of the T-shaped network.

V. SIMULATION RESULTS AND ANALYSIS

To investigate the operation and performance of the resonance- and absorption-based T-shaped impedance matching network design approach, three types of simulations were performed. First, two design examples of the T-shaped matching network were given. The transfer functions of the designed T-shaped matching networks were measured under 1 MHz-100 MHz (broadband). The influence of load-Q on impedance matching performance was investigated. Second, we demonstrate the impedance-matching process for a T-shaped adaptive impedance-matching system. Finally, T-shaped matching networks were operated under four sub-frequency bands to investigate the impedance-matching (power transfer) performance.

A. DESIGN EXAMPLES AND FREQUENCY RESPONSES OF T-SHAPED MATCHING NETWORKS

For a source impedance of $R_s = 50\,\Omega$, and a given inductive access impedance of $Z_{acc} = 75\,\Omega + j25\,\Omega$, Table 1 lists the components values (at $f_0 = 1.6\,MHz$) for various load-Qs.

The frequency responses of the newly-designed T-shaped networks, for various load-Qs, are shown in Fig. 13. For $Z_{acc} = 75\,\Omega$+j25 Ω, according to Eq. (11), the load-Q should be larger than 0.707 (Q_{min}). As in Fig. 13, the T-shaped matching network exhibits a high-pass performance and its bandwidth increases with the reduction of the load-Q. When the load-Q is close to 0.707, e.g., Q = 1, the T-shaped matching network has a relatively flat high-pass behavior. Therefore, to obtain a broader bandwidth of the T-shaped matching network, a smaller load-Q should be selected.

For a source impedance $R_s = 50\,\Omega$, and a capacitive access impedance $Z_{acc} = 30-$j60 Ω, Table 2 lists the component values (at $f_0 = 1.6\,$MHz) for different load-Qs. According to Eq. (14), the load-Q should be greater than 2 (Q_{min}). The transfer functions of the T-shaped matching networks for different load-Qs are shown in Fig. 14. As in Fig. 14, the T-shaped matching network's bandwidth also increases with

TABLE 1. Component values for different load-Qs (Z_{acc} = 75 Ω+j25 Ω).

Z_{acc}	Load-Qs	Component values
Z_{acc}=75 Ω+j25 Ω	10	C_{s1}=199.04pF L_p=27.70uH C_{eq}=156.52pF
	5	C_{s1}=398.09pF L_p=14.31uH C_{eq}=303.32pF
	2	C_{s1}=995.22pF L_p=7.05uH C_{eq}=713.09pF
	1	C_{s1}=1.99nF L_p=6.31uH C_{eq}=1.46nF

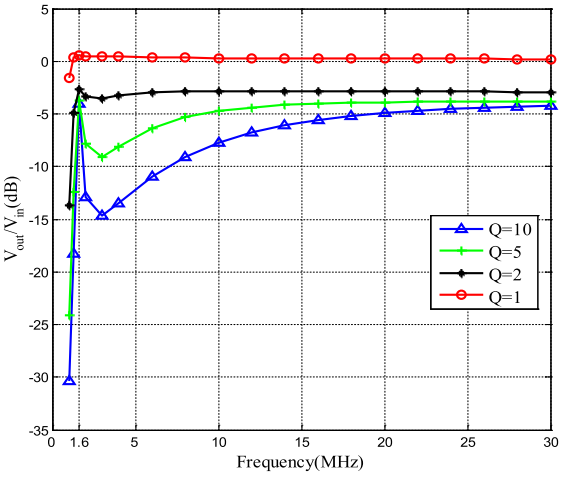

FIGURE 13. The frequency responses for Z_{acc} = 75 Ω + *j*25 Ω.

TABLE 2. Component values for different load-Qs (Z_{acc} = 30 Ω−j60 Ω).

Z_{acc}	Load-Qs	Component values
Z_{acc}=30 Ω-j60 Ω	10	C_{s1}=257.83pF L_p=17.02uH C_{eq}=414.68pF
	8	C_{s1}=322.89pF L_p=13.70uH C_{eq}=552.90pF
	5	C_{s1}=520.92pF L_p=8.80uH C_{eq}=1.11nF
	2.5	C_{s1}=1.09nF L_p=5.0uH C_{eq}=6.63nF

the reduction of the load-Q. We observe that the T-shaped matching network exhibits an overall flat high-pass behavior, in most cases, when the load-Q is near 2.

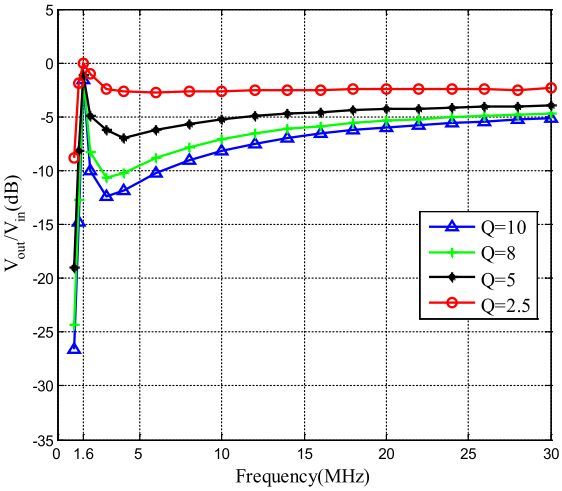

FIGURE 14. The frequency responses for Z_{acc} = 30 Ω−j60 Ω.

B. THE IMPEDANCE MATCHING PROCESS OF THE T-SHAPED ADAPTIVE IMPEDANCE MATCHING SYSTEM

The channel characteristics of VPLC systems have been investigated in [4], [29], where the access impedance was measured under narrowband (0-500 kHz) and broadband (1 MHz-100 MHz) conditions for different vehicles. Form the measurement results, the narrowband transmission system cannot provide reliable connectivity to the VPLC due to the prominent and severe noise interference at low frequencies. Therefore, to evaluate the performance of our adaptive impedance matching system effectively, the simulations were conducted under broadband (1 MHz-100 MHz) conditions.

TABLE 3. Average VPLN access impedance for four frequency bands.

Bands (MHz)	f_c (MHz)	Average impedance (Ω)
7.5-12.5	10	10+j 20
25-35	30	20+j 25
40-60	50	40+j 40
65-95	80	75+j 30

As measured in [3] and [32] (and summarized in [8]), the real part of VPLN access impedance ranges from 0 Ω to 250 Ω, while the imaginary part ranges from −175 Ω to 150 Ω. Table 3 lists the center frequencies (f_c) and the average VPLN access impedance values for four frequency bands. A T-shaped adaptive matching system was designed at 10 MHz (matching frequency) to demonstrate the impedance matching process for Z_{acc} = 10 Ω+j20 Ω.

The impedance-matching process for a T-shaped network is demonstrated in Fig. 15 using a Smith Chart. In this chart, the access impedances as-illustrated abide by the parameters listed in Table 3. The modem (transmitter/receiver) impedance, located at the center of the Smith Chart, is 50 Ω. The four curves (with arrowheads) indicate the complex impedance-matching procedure for Z_{acc} = 10 Ω+j20 Ω. The first negative movement (red curve marked by arrowhead) on the constant resistance circle indicates a series resonant

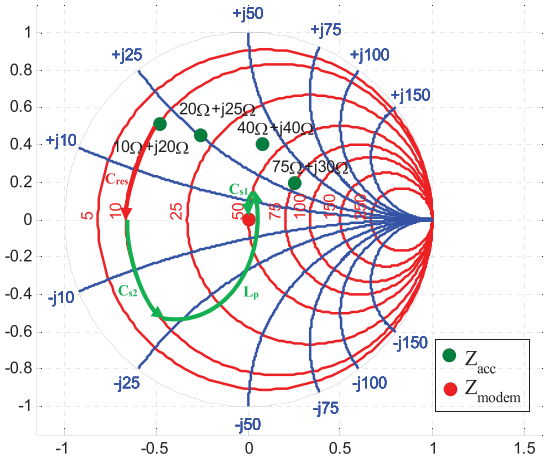

FIGURE 15. The Impedance matching process for a T-shaped network.

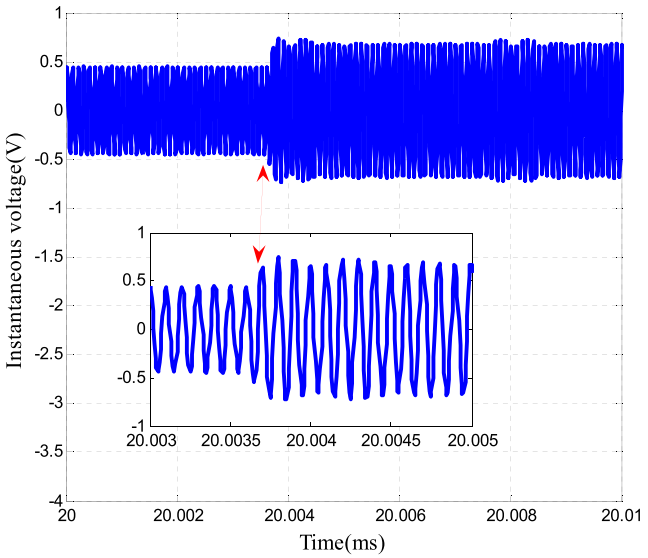

FIGURE 16. The instantaneous voltage of Z_{acc} (Z_{acc} = 10Ω+j20Ω and f_c = 10 *MHz*).

capacitance (C_{res}), which transforms the complex access impedance (10 Ω+j20 Ω) to a real-valued impedance (10 Ω). The other three green curves with arrowheads (C_{s2}, L_p and C_{s1}) represent the real-to-real impedance-matching process shown in Section II-B. The first and second curves with arrowheads (C_{res} and C_{s2}) can be combined into one curve that reflects the series capacitance ($C_{eq} = \frac{C_{res} \times C_{s2}}{C_{res}+C_{s2}}$) in the T-shaped matching network.

Figure 16 exhibits the instantaneous voltage of $Z_{acc} = 10 + \mathrm{j}\,20\,\Omega$ for transmitter-side matching. The voltage and internal impedance of the source were set to 1.414 V_{peak} and 50 Ω in this simulation, respectively. The T-shaped adaptive impedance-matching system was operated at 10 MHz (matching frequency). An 8-bit microcontroller with a lower processing speed was selected for simulation to demonstrate the response time (delay) of the control unit. As shown in Fig. 16, the instantaneous voltage of Z_{acc} increases after 20.0035 ms. This indicates that the T-shaped adaptive impedance-matching system adjusts the component values of the matching network and achieves the impedance matching between the source and the Z_{acc}, thus improving the instantaneous voltage (power) from the source to the VPLN.

C. THE PERFORMANCE OF THE T-SHAPED MATCHING NETWORK

Table 3 shows the center frequencies (f_c) and the average VPLN access impedance values for four frequency bands. Our T-shaped matching networks were designed at f_c (matching frequency) to investigate the impedance matching performance (power transfer) under four frequency bands.

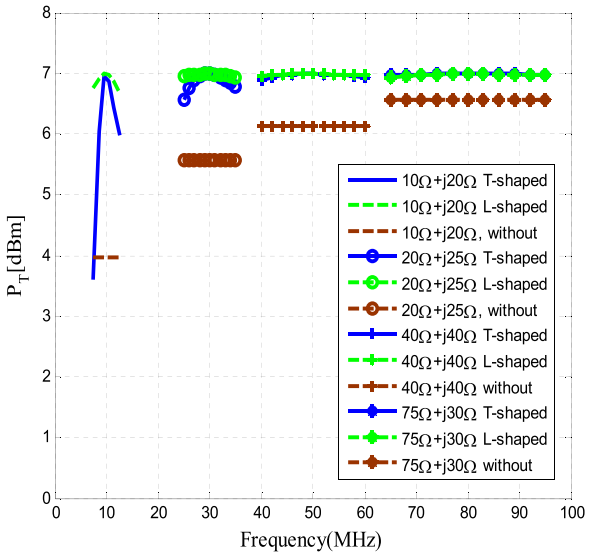

FIGURE 17. Performance for the transmitter-side matching.

1) TRANSMITTER-SIDE MATCHING

For the transmitter-side matching, the voltage and internal impedance of the source were set to 1.414 V_{peak} and 50 Ω, respectively. The average VPLN access impedances for four frequency bands were specified in Table 3. According to Eq. (11) (R_{acc}>R_s) or Eq. (12) (R_{acc}<R_s), a minimum load-Q (Q_{min}) of the T-shaped network can be calculated in every frequency band. To obtain a broader bandwidth of the T-shaped matching network, the smaller load-Q = Q_{min} + 0.1 is selected. The T-shaped matching network was designed according to the resonance- and absorption-based complex impedance-matching approach that was illustrated in Section III-B. The T-shaped matching network deployed between the transmitter (source) and the VPLN access impedances, is operated at f_c for four frequency bands, respectively. When the signal frequency ranges between 1 MHz and 100 MHz, the active power (P_T) that was transferred from the source into the VPLN is measured. The comparative active power performance can be converted to the dBm scale by using the following formula

$$P[dBm] = 10log_{10}(\frac{P}{1mW}). \quad (16)$$

Figure 17 shows the comparative active power performance for various average access impedances. In the simulation, the average VPLN access impedance was set as a constant in every frequency band. Therefore, the power performance of the system without matching network is frequency independent. Our T-shaped matching network was designed at 10 MHz, 30 MHz, 50 MHz and 80 MHz for each of the respective four frequency bands (parameters specified in Table 3). As illustrated in Fig. 17, when the signal frequency is equal to the matching frequency of the T-shaped network, a maximum power transfer (perfect matching) can be achieved. Our T-shaped matching network obtains approximately 3 dB, 1.4 dB, 0.9 dB, and 0.4 dB for the frequencies of 10 MHz, 30 MHz, 50 MHz, and 80 MHz, respectively. Furthermore, even when the signal frequency deviates from the matching frequency, significant signal-power improvements are still achieved by comparing it to the transmission without the matching network. Fig. 17 also shows a performance comparison between the T-shaped and L-shaped matchingnetworks. As shown in Fig. 17, the T-shaped matching network exhibits sensitivity to frequencies (narrow bandwidths) in the lower frequency bands, that is because, according to the expression $Q = \frac{f_0}{BW}$, the bandwidth (BW) of the T-shaped matching network is proportional to the matching frequency (f_0) for a certain load-Q. The load-Q of a T-shaped matching network is always larger than that of an L-shaped network (see Section III-C), so the bandwidths of the T-shaped matching networks are narrower than those of the L-shaped matching networks. However, this is acceptable for simple circuit structure and control logic for impedance adaptation.

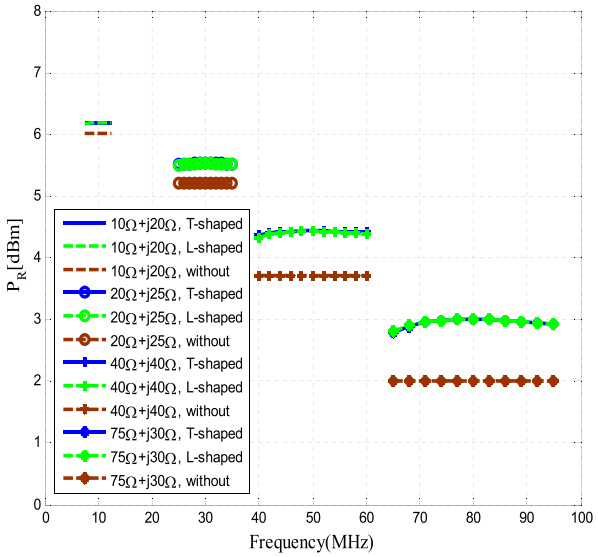

FIGURE 18. Performance for the receiver-side matching.

2) RECEIVER-SIDE MATCHING

The second set of the simulations was made for the receiver-side matching, the V_s and Z_s were also set to 1.414 V_{peak} and 50 Ω, respectively. The input impedance of the receiver was set to 50 Ω. The VPLN access impedances (Z_{acc}) for the four frequency bands are shown in Table 3. In every frequency band, load-Q = Q_{min}+0.1 was imposed on the T-shaped network with a large bandwidth. The designed T-shaped matching network deployed between the VPLN and receiver, was operated at f_c, and the active power (P_R) extracted from the VPLN into the receiver was measured and converted to the dBm scale using Eq. (16).

The active power performance of the four frequency bands for the receiver-side matching is shown in Fig. 18. As shown in Fig. 18, our T-shaped matching network exhibits a fairly flat in-band behavior, which shows almost the same excellent impedance matching performance as the L-shaped matching network. Even when the signal frequency deviates from the operating frequency (matching frequency), our T-shaped matching network also significantly improves the signal power transfer over a wide range of values around the operating frequency. There are approximate gains of 0.2 dB, 0.3 dB, 0.7 dB, and 1.0 dB, respectively, for the four frequency bands.

VI. CONCLUSION

In this paper, a T-shaped adaptive impedance matching system was designed; the system includes a measurement unit, control unit and impedance matching unit. The details about the T-shaped adaptive matching system were presented, and the performance of the system, under various power line conditions, was evaluated via simulations. The results demonstrate that the T-shaped adaptive impedance matching system can significantly improve signal power transfer.

To investigate the influence of insertion loss on the impedance matching network, the next phase of our research will investigate parasitic-aware three-element impedance matching networks.

REFERENCES

[1] H. C. Ferreira, L. Lampe, J. Newbury, and T. G. Swart, *Power Line Communications: Theory and Applications for Narrowband and Broadband Communications over Power Lines*. Hoboken, NJ, USA: Wiley, 2010.

[2] T. Huck, J. Schirmer, T. Hogenmuller, "Tutorial about the implementation of a vehicular high speed communication system," in *Proc. Int. Symp. Power Line Commun. Appl.*, Vancouver, BC, Canada, Apr. 2005, pp. 162–166.

[3] N. Taherinejad, R. Rosales, L. Lampe, and S. Mirabbasi, "Channel characterization for power line communication in a hybrid electric vehicle," in *Proc. IEEE Int. Symp. Power Line Commun. Appl.*, Mar. 2012, pp. 328–333.

[4] M. Mohammadi, L. Lampe, M. Lok, S. Mirabbasi, M. Mirvakili, R. Rosales, and P. van Veen, "Measurement study and transmission for in-vehicle power line communication," in *Proc. IEEE Int. Symp. Power Line Commun. Appl.*, Dresden, Germany, Mar. 2009, pp. 73–78.

[5] S. Barmada, M. Raugi, M. Tucci, and T. Zheng, "Power line communication in a full electric vehicle: Measurements, modelling and analysis," in *Proc. ISPLC*, 2010, pp. 331–336.

[6] V. Degardin, M. Lienard, P. Degauque, E. Simon, and P. Laly, "Impulsive noise characterization of in-vehicle power line," *IEEE Trans. Electromagn. Compat.*, vol. 50, no. 4, pp. 861–868, Nov. 2008.

[7] L. Zhang, H. Ma, D. Shi, P. Wang, G. Cai, and X. Liu, "Reliability oriented modeling and analysis of vehicular power line communication for vehicle to grid (V2G) information exchange system," *IEEE Access*, vol. 5, pp. 12449–12457, 2017.

[8] N. Taherinejad, L. Lampe, and S. Mirabbasi, "An adaptive impedance-matching system for vehicular power line communication," *IEEE Trans. Veh. Technol.*, vol. 66, no. 2, pp. 927–940, Feb. 2017.

[9] P. A. Janse van Rensburg and H. C. Ferreira, "Coupler winding ratio selection for effective narrowband power-line communications," *IEEE Trans. Power Del.*, vol. 23, no. 1, pp. 140–149, Jan. 2008.
[10] S. Stiri, A. Chaoub, T. E. Maliki, and R. Osseni, "Realization of a low-cost impedance matching circuit for stable power line communications: From testbeds to practical implementation," in *Proc. 19th IEEE Medit. Electrotech. Conf. (MELECON)*, May 2018, pp. 219–224.
[11] M. P. Sibanda, P. A. Janse van Rensburg, and H. C. Ferreira, "Impedance matching with low-cost, passive components for narrowband PLC," in *Proc. IEEE Int. Symp. Power Line Commun. Appl.*, Apr. 2011, pp. 335–340.
[12] M. P. Sibanda, P. A. J. van Rensburg, and H. C. Ferreira, "A compact economical PLC band-pass coupler with impedance matching," in *Proc. IEEE 17th Int. Symp. Power Line Commun. Appl.*, Mar. 2013, pp. 339–344.
[13] P. A. Janse van Rensburg, M. P. Sibanda, and H. C. Ferreira, "Integrated impedance-matching coupler for smart building and other power-line communications applications," *IEEE Trans. Power Del.*, vol. 30, no. 2, pp. 949–956, Apr. 2015.
[14] M. Antoniali, M. De Piante, and A. M. Tonello, "PLC noise and channel characterization in a compact electrical car," in *Proc. IEEE 17th Int. Symp. Power Line Commun. Appl.*, Mar. 2013, pp. 29–34.
[15] C.-Y. Park, K.-H. Jung, and W.-H. Choi, "Coupling circuitary for impedance adaptation in power line communications using VCGIC," in *Proc. IEEE Int. Symp. Power Line Commun. Appl.*, Apr. 2008, pp. 293–298.
[16] P. R. Chin, A. K. M. Wong, K. I. Wong, and N. Barsoum, "Modelling of LCRC adaptive impedance matching circuit in narrowband power line communication," in *Proc. IEEE 11th Int. Conf. Power Electron. Drive Syst.*, Jun. 2015, pp. 132–135.
[17] N. Taherinejad, L. Lampe, and S. Mirabbasi, "Adaptive impedance matching for vehicular power line communication systems," in *Proc. 18th IEEE Int. Symp. Power Line Commun. Appl.*, Mar./Apr. 2014, pp. 214–219.
[18] Q. Gu, J. R. De Luis, A. S. Morris, and J. Hilbert, "An analytical algorithm for pi-network impedance tuners," *IEEE Trans. Circuits Syst. I, Reg. Papers*, vol. 58, no. 12, pp. 2894–2905, Dec. 2011.
[19] A. van Bezooijen, M. A. de Jongh, F. van Straten, R. Mahmoudi, and A. van Roermund, "Adaptive impedance-matching techniques for controlling L networks," *IEEE Trans. Circuits Syst. I, Reg. Papers*, vol. 57, no. 2, pp. 495–505, Feb. 2010.
[20] B. Wang and Z. Cao, "A review of impedance matching techniques in power line communications," *Electronics*, vol. 8, no. 9, p. 1022, 2019.
[21] M. Thompson and J. K. Fidler, "Determination of the impedance matching domain of impedance matching networks," *IEEE Trans. Circuits Syst. I, Reg. Papers*, vol. 51, no. 10, pp. 2098–2106, Oct. 2004.
[22] Y. Sun and J. K. Fidler, "Design of Π impedance matching networks," in *Proc. IEEE Int. Symp. Circuits Syst.*, May/Jun. 1994, pp. 5–8.
[23] M. Schmidt, E. Lourandakis, and A. Leidl, "A comparison of tunable ferroelectric Π- and T-matching networks," in *Proc. Eur. Microw. Conf.*, Oct. 2007, pp. 98–101.
[24] B. K. Chung, "Q-based design method for t network impedance matching," *Microelectron. J.*, vol. 37, no. 9, pp. 1007–1011, Sep. 2006.
[25] R. Liao, J. Tan, and H. Wang, "Q-based design method for impedance matching network considering load variation and frequency drift," *Microelectron. J.*, vol. 42, no. 2, pp. 403–408, Feb. 2011.
[26] A. K. Ar, S. G. Singh, and A. Dutta, "Analytical design technique for real-to-real single- and dual-frequency impedance matching networks in lossy passive environment," *IET Microw., Antennas Propag.*, vol. 12, no. 6, pp. 1013–1020, May 2018.
[27] M. Bozanic and S. Sinha, *Power Amplifiers for the S-, C-, X- and Ku-bands: An EDA Perspective*. Cham, Switzerland: Springer, 2015.
[28] C. Bowick, J. Blyler, and C. Ajluni, *RF Circuit Design*. Amsterdam, The Netherlands: Elsevier, 2008.
[29] A. Pittolo, M. De Piante, F. Versolatto, and A. M. Tonello, "In-vehicle power line communication: Differences and similarities among the in-car and the in-ship scenarios," *IEEE Veh. Technol. Mag.*, vol. 11, no. 2, pp. 43–51, Jun. 2016.
[30] G.-Y. Zhang, Y.-J. Dai, X.-X. Zhang, and Y.-J. Lv, "Adaptive impedance matching system for downlink of passive semi-ultra wideband ultra-high frequency radio frequency identification tag," *Int. J. Adapt. Control Signal Process.*, vol. 26, no. 6, pp. 530–540, Jun. 2012.
[31] S. Franco, *Design With Operational Amplifiers And Analog Integrated Circuits*. New York, NY, USA: McGraw-Hill, 2002.
[32] N. Taherinejad, R. Rosales, S. Mirabbasi, and L. Lampe, "A study on access impedance for vehicular power line communications," in *Proc. IEEE Int. Symp. Power Line Commun. Appl.*, Apr. 2011, pp. 440–445.

BINGTING WANG (Graduate Student Member, IEEE) received the B.S. degree in physics and the M.S. degree in communication and information system from Anhui University, Hefei, in 2008 and 2011, respectively. He is currently pursuing the Ph.D. degree with the Department of Telecommunication and Information Engineering, Nanjing University of Posts and Telecommunications, Nanjing, China.

Since 2015, he has been a Lecturer with the College of Mechanical and Electrical Engineering, Chuzhou University. His research interests include power line communications and its applications.

ZIPING CAO received the B.S. and M.S. degrees in materials science and engineering from the Kunming University of Science and Technology, Kunming, in 2002, and the Ph.D. degree in materials physics and chemistry from the Chinese Academy of Sciences, Shanghai, in 2005.

From 2005 to 2007, he was a JSPS Postdoctoral Fellow with the Graduate School of Engineering, Nagoya University, Nagoya, Japan. From 2009 to 2011, he was an Assistant Professor with the Graduate School of Engineering, Tohoku University, Sendai, Japan. Since 2012, he has been a Professor with the School of Telecommunication and Information Engineering, Nanjing University of Posts and Telecommunications, Nanjing, China. He has authored of more than 70 articles and 20 inventions. His research interests include power line carrier communication, wireless sensor networks, environmental energy harvesting, and contactless energy transferring.

FEI SONG received the B.S. degree in communication engineering from the North China Institute of Aerospace Engineering, Langfang, in 2016. She is currently pursuing the M.S. degree with the Department of Telecommunication and Information Engineering, Nanjing University of Posts and Telecommunications, Nanjing, China. Her research interests include power line communications and its applications.